Journal of Organometallic Chemistry 694 (2009) 3570–3579

Contents lists available at ScienceDirect

Journal of Organometallic Chemistry

journal homepage: www.elsevier.com/locate/jorganchem

Synthesis, and characterization of ruthenium(II) polypyridyl complexes containing α-amino acids and its DNA binding behavior

Prashant Kumar [a], Ashish Kumar Singh [a], Jitendra Kumar Saxena [b], Daya Shankar Pandey [a,*]

[a] Department of Chemistry, Faculty of Science, Banaras Hindu University, Varanasi 221 005, UP, India
[b] Division of Biochemistry, Central Drug Research Institute, Chattar Manzil, P.O. Box 173, Lucknow 226 001, UP, India

ARTICLE INFO

Article history:
Received 6 June 2009
Received in revised form 1 July 2009
Accepted 6 July 2009
Available online 3 August 2009

Keywords:
Ruthenium complexes
Polypyridyl
Topoisomerase
Heme polymerase

ABSTRACT

Reactivity of the ruthenium complexes $[Ru(\kappa^3\text{-tptz})(PPh_3)Cl_2]$ (**1**) and $[Ru(\kappa^3\text{-tpy})(PPh_3)Cl_2]$ (**2**) [tptz = 2,4,6-tris(2-pyridyl)-1,3,5-triazine; tpy = 2,2′:6′,2″-terpyridine] with several α-amino acids [glycine (gly); leucine (leu); isoleucine (isoleu); valine (val); tyrosine (tyr); proline (pro) and phenylalanine (phe)] have been investigated. Cationic complexes with the general formulations $[Ru(\kappa^3\text{-L})(\kappa^2\text{-L}'')(PPh_3)]^+$ (L = tptz or tpy; L″ = gly, leu, isoleu, val, tyr, pro, and phe] have been isolated as tetrafluoroborate salts. The resulting complexes have been thoroughly characterized by analytical, spectral and electrochemical studies. Molecular structures of the representative complexes $[Ru(\kappa^3\text{-tptz})(val)(PPh_3)]BF_4$ (**6**), $[Ru(\kappa^3\text{-tpy})(leu)(PPh_3)]BF_4$ (**10**) and $[Ru(\kappa^3\text{-tpy})(tyr)(PPh_3)]BF_4$ (**13**) have been determined crystallographically. The complexes $[Ru(\kappa^3\text{-tptz})(leu)(PPh_3)]BF_4$ (**4**), $[Ru(\kappa^3\text{-tptz})(val)(PPh_3)]BF_4$ (**6**), $[Ru(\kappa^3\text{-tpy})(leu)(PPh_3)]BF_4$ (**10**) $[Ru(\kappa^3\text{-tpy})(tyr)(PPh_3)]\ BF_4{\cdot}3H_2O$ (**13**) exhibited DNA binding behavior and acted as mild Topo II inhibitors (10–40%). The complexes also inhibited heme polymerase activity of the malarial parasite *Plasmodium yoelii* lysate.

1. Introduction

Ruthenium(II) polypyridyl complexes have drawn immense research interest over past couple of decades due to their interesting photophysical and photochemical properties that makes them potentially useful in diverse areas [1–5]. Owing to intense MLCT luminescence, excited state redox properties and ability to bind DNA, Ru(II) polypyridyl complexes serve as promising DNA probes [6,7]. Ligands present in the complexes play an important role in determining and improving light emitting and electron-transfer performances [8–10]. Ru(II) complexes may bind DNA through non-covalent interactions such as electrostatic binding, groove binding and intercalation [11,12]. Many of the complexes bind DNA through a combination of binding modes that is dependent on the structural characteristics of compounds. An understanding of how the metal complexes bind DNA will not only pave the way to understand fundamentals of these interactions but also, about the variety of potential applications [13–16].

It has been observed that the complexes $[Ru(\kappa^3\text{-L})(EPh_3)Cl_2]$ (E = P, As; L = tpy and tptz) containing both the EPh_3 and polypyridyl ligands behave as good precursors and act as metallo-ligands in the syntheses of homo-/hetero-bimetallic complexes [17,18]. Also, these behave as inhibitors of Topo II and heme polymerase activity. Further, the chemistry of transition metal complexes containing α-amino acids has been of significant interest [19,20]. The synthesis of complexes containing α-amino acids has become increasingly important due to their significant role in biological fields [19,20]. The amino acids are known to bind metal ions as a bi-dentate N,O-donor ligand forming five membered chelate rings after dissociation of the acidic proton [17,18]. It is noteworthy that while the chemistry of many transition metal complexes containing amino acids has been studied in detail, the chemistry of ruthenium complexes has received only little attention [21,22]. Furthermore, DNA topoisomerases which are intricately involved in maintaining the topographic structure of DNA transcription and mitosis, have been identified as an important biochemical target in cancer chemotherapy, microbial infections and in the development of anti-filarial compounds [23–25]. Recently, ruthenium(II) complexes based on polypyridyl and pyridyl-azine ligands as inhibitors of Topo II activity were reported [23–26]. It has been shown that the inhibition percentage largely depends on nature of the complexes, ligands involved and the presence of uncoordinated sites on polypyridyl ligands.

In addition, the complexes containing polypyridyl ligands like tptz or tpy and α-amino acids along with EPh_3 are yet to be explored. It was felt that incorporation of bio-relevant ligands like amino acids in the complexes may lead to significant changes in their properties. With this aim we have synthesized new cationic complexes $[Ru(\kappa^3\text{-L})(\kappa^2\text{-}O,N\text{-L}')(PPh_3)]^+$ [(L = tptz or tpy and L′ = α-amino acids [glycine (gly); leucine (leu); isoleucine (isoleu); valine (val); tyrosine (tyr); proline (pro) and phenylalanine

* Corresponding author. Tel.: +91 542 2307321 105.
E-mail address: dspbhu@bhu.ac.in (D.S. Pandey).

0022-328X/$ - see front matter © 2009 Elsevier B.V. All rights reserved.
doi:10.1016/j.jorganchem.2009.07.014

(phe)] containing amino acids. In this paper we report reproducible synthesis of the mixed-ligand polypyridyl ruthenium complexes imparting 2,4,6-tris(2-pyridyl)-1,3,5-triazine (tptz), 2,2′:6′,2″-terpyridine (tpy) and α-amino acids. We also describe herein inhibitory activity of the complexes on DNA–Topoisomerase II of the filarial parasite *S. cervi* and β-hematin/hemozoin formation in the presence of *Plasmodium yoelii* lysate.

2. Results and discussion

The reactions of [Ru(κ^3-L)(EPh$_3$)Cl$_2$] (E = P, As; L = tpy or tptz) with α-amino acids (glycine, leucine, isoleucine, valine, tyrosine, proline and phenylalanine) in methanol in presence of a base (KOH) under refluxing conditions afforded cationic complexes [Ru(κ^3-tptz)(gly)(PPh$_3$)]BF$_4$ (**3**), [Ru(κ^3-tptz)(leu)(PPh$_3$)]BF$_4$ (**4**), [Ru(κ^3-tptz)(isoleu)(PPh$_3$)]BF$_4$ (**5**), [Ru(κ^3-tptz)(val)(PPh$_3$)]BF$_4$ (**6**), [Ru(κ^3-tptz)(tyr)(PPh$_3$)]BF$_4$ (**7**), [Ru(κ^3-tptz)(pro)(PPh$_3$)]BF$_4$ (**8**), [Ru(κ^3-tpy)(gly)(PPh$_3$)]BF$_4$ (**9**), [Ru(κ^3-tpy)(leu)(PPh$_3$)]BF$_4$ (**10**), [Ruκ^3-tpy)(isoleu)PPh$_3$)]BF$_4$ (**11**), [Ru(κ^3-tpy)(val)(PPh$_3$)]BF$_4$ (**12**), [Ru(κ^3-tpy)(tyr)(PPh$_3$)]BF$_4$ (**13**), [Ru(κ^3-tpy)(pro)(PPh$_3$)]BF$_4$ (**14**) and [Ru(κ^3-tpy)(phe)(PPh$_3$)]BF$_4$ (**15**) in excellent yields. The complexes have been isolated as tetrafluoroborate salt. A simple scheme showing syntheses of the complexes is depicted in Scheme 1.

The complexes have been characterized by satisfactory elemental analyses, spectral and electrochemical studies. Analytical data of the complexes under study conformed well to their respective formulations. Information about composition of the complexes has also been obtained by FAB-MS spectral studies. FAB-MS spectra of representative complexes **7** and **13** are shown in Fig. 1, and resulting data with their assignments are recorded in the Section 3.

Infrared spectra of [**3**] BF$_4$–[**8**]BF$_4$ exhibited sharp and strong bands at ~1630 and ~1390 cm^{-1}, while those of [**9**] BF$_4$–[**15**]BF$_4$ showed bands at ~1610 and ~1380 cm^{-1}, respectively. These bands has been assigned to ν_{as}(CO) and ν_s(CO) stretching vibrations of the coordinated carboxylate group [27]. The bands at ~3300 cm^{-1} has been assigned to N–H stretching vibrations ν(N–H). The vibrations due to counter ion BF_4^- and PF_6^- appeared at ~1055 and 840 cm^{-1} in the IR spectra of respective complexes [28,29].

The ^{1}H and ^{31}P NMR spectra of complexes were recorded in CDCl$_3$ and spectral data are summarized in the experimental section. Shift in the position of signals associated with protons of tptz and tpy, suggested coordination of amino acids to the metal centre ruthenium in bi-dentate fashion [26]. The position and integrated intensity of various signals corresponding to tptz corroborated to a system involving coordination of tptz with ruthenium in κ^3-manner with two magnetically equivalent coordinated pyridyl and one uncoordinated pyridyl rings [30]. Well resolved signals associated with coordinated amino acids appeared in ^{1}H NMR spectra of the respective complexes. The aromatic protons (12) corresponding to pyridyl rings of tptz in [**3**] BF$_4$–[**8**] BF$_4$, resonated in the range δ 7.48–8.95 ppm. Further, this region displayed overlapping signals arising from protons of the uncoordinated pyridyl ring. The aromatic protons of triphenylphosphine in the complexes [**3–15**] BF$_4$ resonated at ~δ 7.02–7.32 ppm as a broad multiplet.

In the ^{1}H NMR spectrum of complex **15** signals corresponding to phenyl ring protons (two) of phenylalanine merged with broad multiplet associated with aromatic protons of PPh$_3$. Similar observation has been made in the case of [**7**] BF$_4$ and [**13**] BF$_4$, where phenyl ring protons of the tyrosine resonated as doublet at δ 6.88 and 6.57 and δ 6.85 and 6.54 ppm, respectively. Main feature

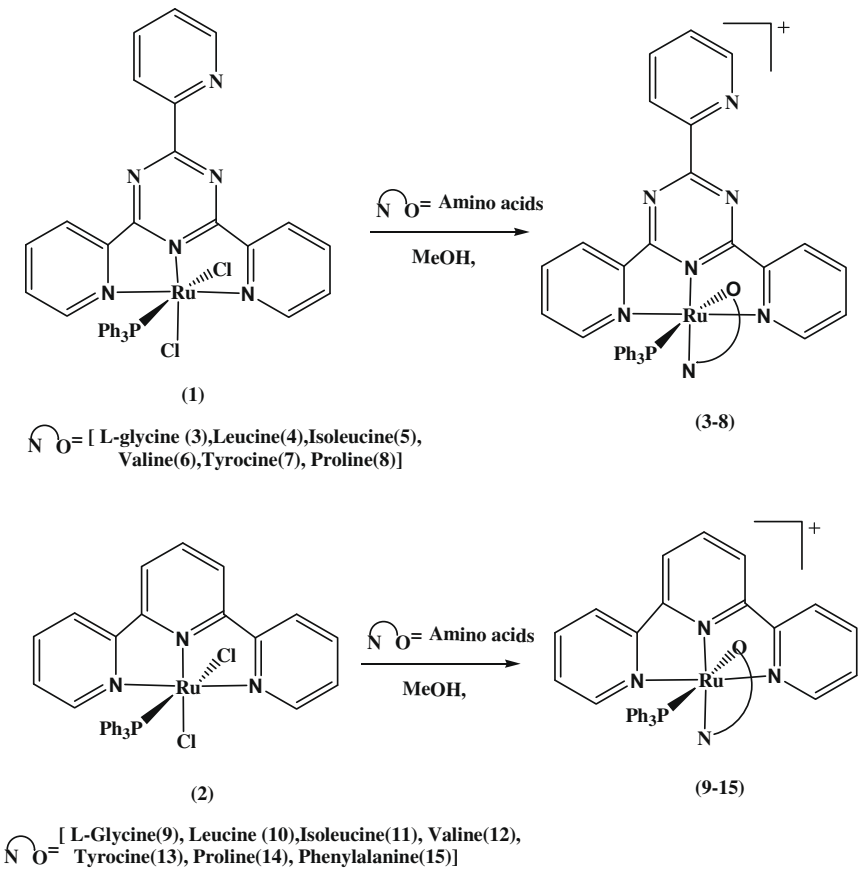

Scheme 1.

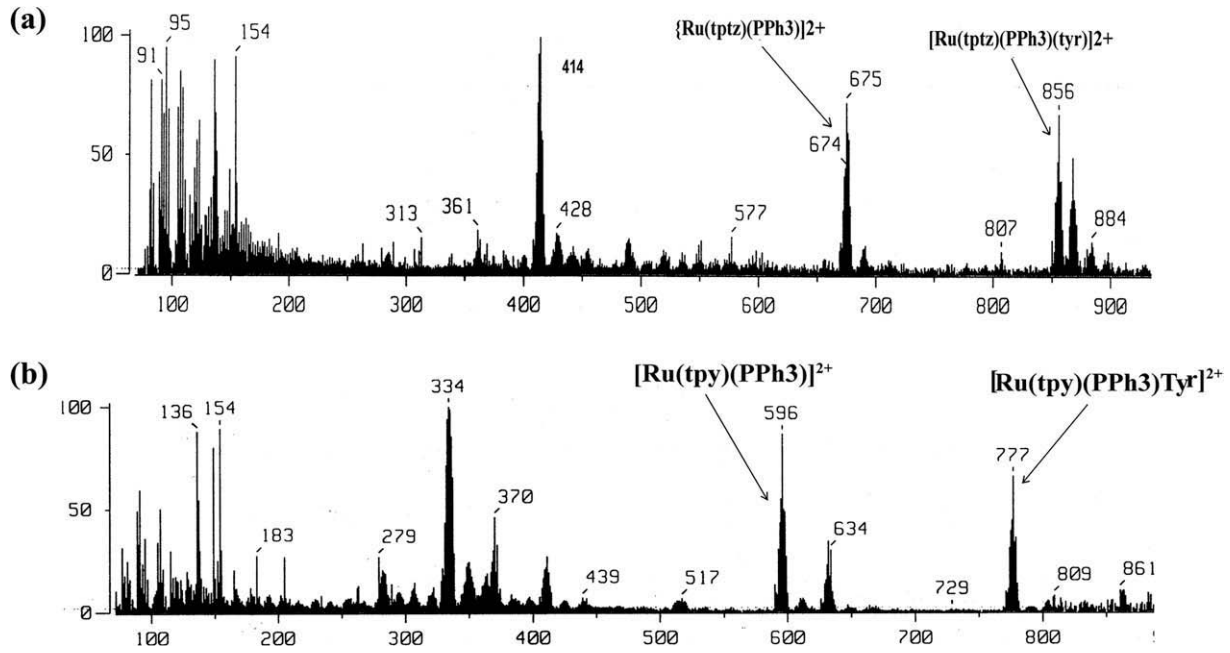

Fig. 1. FAB-MS spectra with peak assignment for **7** (a) and **13** (b).

of the ^{1}H NMR spectra of all the complexes containing amino acids is the presence of multiplets and doublets in low-frequency side for methyl, methylene, methene and coordinated NH_2 protons of the amino acids. In $^{31}P\{^1H\}$ NMR spectra of the complexes [**3**] BF_4–[**8**] BF_4, the ^{31}P nuclei of coordinated PPh_3 resonated as a sharp singlet in the range δ 40.77–39.01 ppm while, it resonated at $\sim\delta$ 45.38–43.30 ppm and for [**9**] BF_4 to [**15**] BF_4, as sharp singlet in the high-frequency side in comparison to that in the tptz containing complexes.

The complexes under study displayed absorptions in the visible and ultraviolet region. UV–Visible spectral data of the complexes **3–15** are recorded in experimental section and representative spectra for [**3**] BF_4–[**8**] BF_4 and [**9**] BF_4–[**15**] BF_4 is depicted in Fig. 2a and b. Electronic spectra of these complexes exhibited intense absorptions in the UV region due to π–π^* intra-ligand charge-transfer (ILCT) transitions, together with broad $d_{Ru(II)}$ to $\pi^*_{(L)}$ pyridyl MLCT bands in the visible region. On the basis of its position and intensity the lowest energy absorption bands at $\sim$490 nm in the spectra of the complexes [**3**]BF_4–[**8**]BF_4 containing amino acids have been assigned to $d\pi_{(Ru)} \rightarrow \pi^*_{(tptz)}$ MLCT transitions, while the one in high energy side at $\sim$350, 276–297 and $\sim$240 nm to the intra-ligand $\pi \rightarrow \pi^*/n \rightarrow \pi^*$ transitions. Red shifting in the position of MLCT bands in the complexes containing amino acids may be attributed to greater π back bonding.

Further, the complexes containing tpy displayed a red shift in the position of lowest energy absorption bands at $\sim$500 nm for [**9**] BF_4–[**15**] BF_4 in comparison to the tptz complexes. It may be attributed to the greater stabilization of π^* orbitals on tpy ligand relative to tptz. The main feature of the UV spectra of the complexes containing amino acids is a decrease in the absorbance with a decrease in molecular weight of the amino acids. The intense absorption bands in the ultraviolet region has been assigned to intra-ligand transitions The absorptions in the visible region are rather weak and are probably due to ligand-field transitions [31,32].

Electrochemical properties of the complexes **3**, **5**, and **13** were followed by cyclic voltammetry in acetonitrile solution (0.1 M TBAP) at room temperature (scan rate 100 mV/s). Resulting data is summarized in Table 1 and selected voltammograms are shown

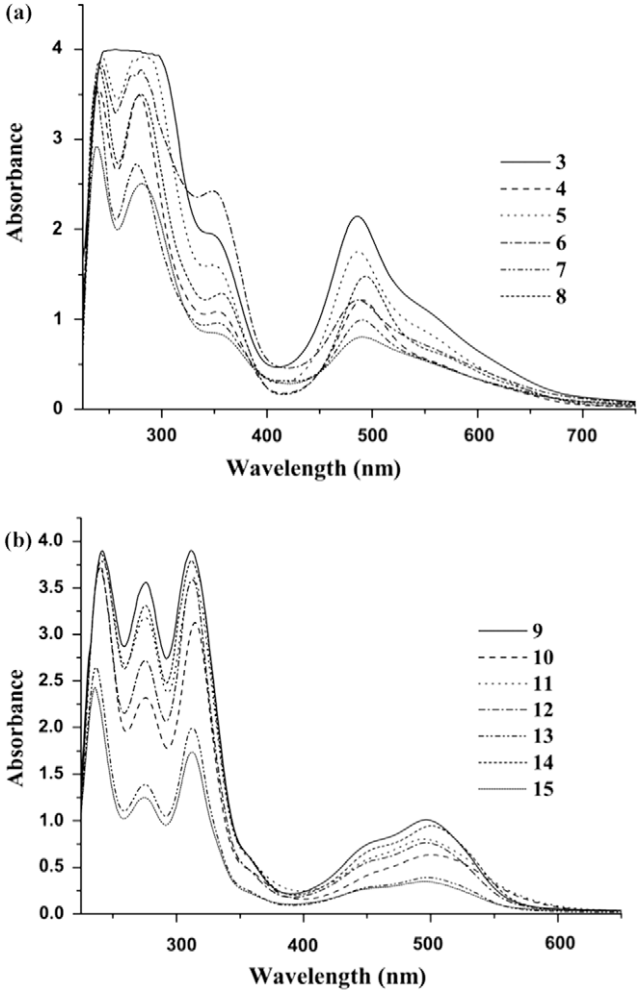

Fig. 2. UV–Vis spectra molecular complexes **3**–**8** (a) and **9**–**15** (b) in dichloromethane.

Table 1
Cyclic voltammetric data for mononuclear ruthenium(II) complexes.

Complexes	E^0_{ox}, V (ΔE, mV)	E^0_{ox}, V (ΔE, mV)
3	0.37(76)	−1.07, −1.86
5	0.525(49)	−1.09, −1.79
13	0.530(58)	−1.06, −1.61

in Fig. S4. The complexes **3**, **5**, and **13** exhibited an oxidative potential in the range 0.30–0.55 V vs. glassy carbon electrode, which is assigned to Ru(II)/Ru(III) oxidation. The peak-to-peak separation (ΔEp) of ~100 mV and the fact that anodic peak current (i_{pa}) is almost equal to the cathodic peak current (i_{pc}), suggested for a reversible electron-transfer process. One-electron nature of the oxidation was established by comparing its current height with that of standard ferrocene/ferrocenium couple under identical experimental conditions. The magnitudes of the oxidation potential indicate that the bivalent state of ruthenium is comfortable in this N, O and P coordination sphere. Further, Ru(II)/Ru(III) oxidation potential in the complexes $[Ru(\kappa^3\text{-}L)(\kappa^2\text{-}L'')(PPh_3)]BF_4$, (L = tptz, tpy; L″ = α-amino acids) is lower than that in $[Ru(\kappa^3\text{-}L)(PPh_3)Cl_2]$ (0.70 V). It suggested that the anions resulting from α-amino acids are better stabilizers of the trivalent state of ruthenium compared to tptz/tpy, An interesting feature of the cyclic voltammetry of complexes **3, 5**, and **13** is an increase in the positive potential as the molecular weight of amino acid increases. Successive two-electron reductions were displayed by all the complexes, at ~1.07–1.09 and 1.69–1.86 V in case of the tptz and 0.56–0.77 and 1.11–1.69 V in case of tpy complexes. For both the tptz Ru^{2+} and tpy Ru^{2+} series, coordinated ligands with a higher number of the nitrogen atoms result in more anodic oxidation potentials (Table 1). It is consistent with the earlier studies showing that as ligand becomes more electron deficient there is concomitant lowering of the ligand LUMO resulting in an enhanced π acceptor properties and more anodic $Ru^{III/II}$ oxidation couples [32]. The first ligand-based reduction also reflects the relative electron deficiency within in a series with couples becoming more facile as number of the nitrogen atom increases in the ligand.

Molecular structures of the complexes **6**, **10** and **13** have been determined crystallographically (Figs. 3–5). Details about data collection, solution and refinement are recorded in Table 2 and important geometrical parameters are summarized in Table 3. A common structural feature of the complexes **6**, **10**, and **13** is the arrangement of various ligands about the metal centre. In these complexes two of the coordination sites about the metal centre are occupied by N7–O1, N4–O1, N2–O1 from the amino acids, one position by P1 of the coordinated PPh_3 and along with tptz/tpy coordinated in κ^3-manner. The angles N1–Ru–N2 and N2–Ru–N3 **6** and **13** are essentially equal and are 79.07(19) (**6**), 78.70(18) (**6**), 79.9(3) (**13**) and 79.4(2)° (**13**), whereas in **10** these are 79.3(3) and 79.4(3)°, respectively. It suggested an inward bending of the coordinated pyridyl group and it may be the reason for observed octahedral distortion [24]. Further, the distortion from regular octahedral geometry is supported by intra-ligand *trans* angles N1–Ru–N3 in **6, 13**, and **10** (Table 3). The Ru1 to central triazine nitrogen bond length Ru1–N2 in **6** is 1.936(4) Å, which is shorter than Ru1 to coordinated pyridyl nitrogen bond lengths Ru1–N1 [2.101(5) Å] and Ru1–N3 [2.090(5) Å]. The Ru–N bond lengths Ru1–N2, Ru1–N1 and Ru1–N3 are 2.12(2), 2.167(19), and 1.94(2) Å in **10**, while these are 1.951(5), 2.075(6) and 2.072(6) Å, in **13**. The Ru–N bond distances are consistent with κ^3-coordination of the tptz/tpy and comparable to those in other Ru^{II} tptz/tpy complexes [24,25,33]. The uncoordinated pyridyl ring in **6** is inclined at 18.6° from the central triazine ring plane.

Crystal structures of **6**, **13**, and **10** revealed the presence of extensive intra- and intermolecular C–H···X (X = N, Cl, and F) and

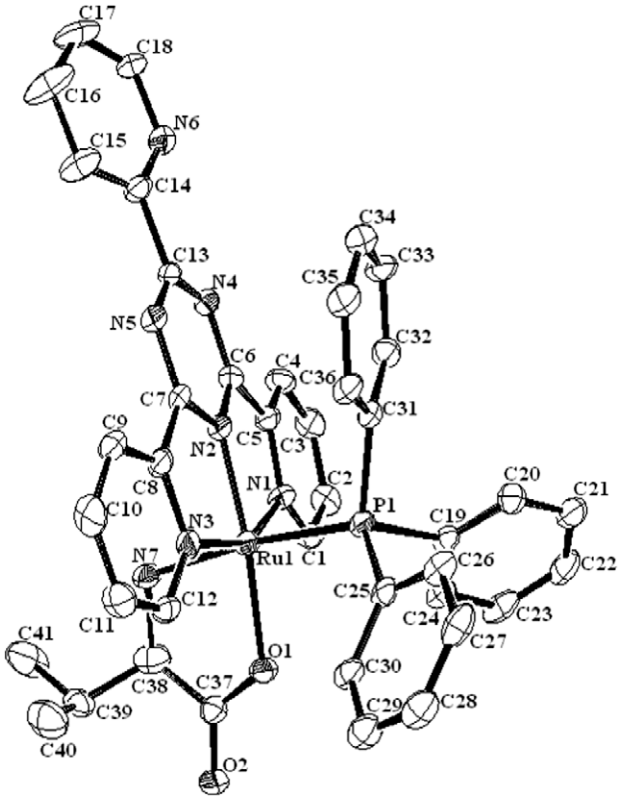

Fig. 3. Molecular structure of **6**.

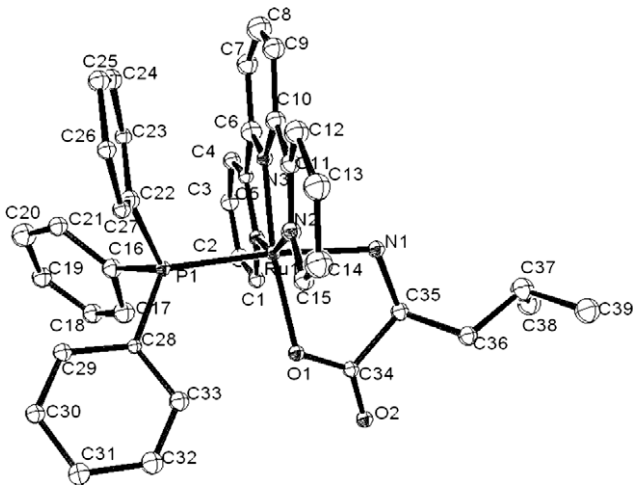

Fig. 4. Molecular structure of **10**.

C–H···π interactions. These types of interactions play significant role in building huge supramolecular moieties [34–36]. The matrices for various weak interactions are recorded in Table S1 and the motifs resulting thereof are depicted in Figs. S5–S7. Weak interaction studies in **6** displayed face to face C–H···π interactions leading to formation of straight chains, which are interlinked to another chain through C–H···N interactions. Interestingly, in **13** parallelogram-shaped water hexamers aggregated into tape like infinite water chain (Fig. 6). On one side of the water chain water molecules (O1w, O2w, O3w) are connected into infinite one dimensional water chain in ABC fashion through strong hydrogen-bonding interactions. The O···O distances are in the range of 2.792–2.892 Å [O1w···O2w(2.823); O2w···O3w(2.892); O3w···O1w(2.792)], and

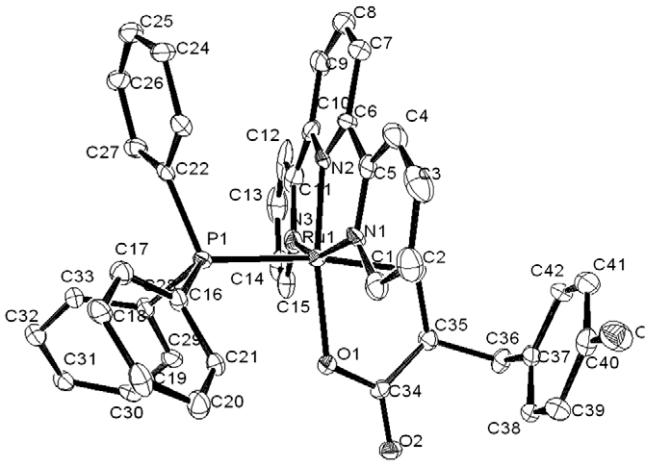

Fig. 5. Molecular structure of **13**.

Table 2
Crystal data for complexes **6**, **10** and **13**.

Complexes	**6**	**10**	**13**
Chemical formula	$C_{41}H_{35}O_2F_4N_7PBF_4Ru$	$C_{42}H_{47}BF_4N_4O_3PRu$	$C_{39}H_{38}ClN_4O_2PRu$
Formula weight	876.61	874.69	833.13
Color, habit	Dark red, block	Dark brown, block	Dark red, block
Crystal size (mm)	0.33 × 0.27 × 0.21	0.38 × 0.34 × 0.31	0.36 × 0.34 × 0.31
Space group	*P*212121	$P\bar{2}12121$	*P*21
Cryst system	Orthorhombic	Orthorhombic	Monoclinic
a (Å)	12.5482(3)	10.8288(9)	12.1446(16)
b (Å)	14.3005(3)	12.6184(10)	9.7376(12)
c (Å)	21.5070(7)	31.197(2)	16.401(2)
α (°)	90	90.00	90.00
β (°)	90	90	101.857(2)
γ (°)	90	90	90.00
V (Å^3)	3859.34(18)	4262.8(6)	1898.2(4)3
Z	4	4	3
D_{calc} (g cm^{-3})	1.509	1.363	2.218
μ (mm^{-1})	0.514	0.465	1.061
T (K)	150(2)	293(2)	293(2)
Number of reflections	6280	10 528	6877
Number of parameters	517	519	464
R factor all	0.0581	0.0899	0.0834
R factor [$I > 2\sigma(I)$]	0.0441	0.0727	0.0674
WR_2	0.1261	0.2585	0.2109
WR_2 [$I > 2\sigma(I)$]	0.1118	0.2151	0.1722
Goodness-of-fit (GOF)	1.037	1.052	1.431

hydrogen-bonded O···O···O angles ranges from 87.86° (O2w···O3w···O1w) to 124.01° (O1w···O3w···O1w). Both the distances and angles are in the range reported in ice and water clusters [37–39].

Change in the electrophoretic mobility of plasmid DNA on agarose gel is commonly taken as evidence for direct DNA–metal interactions. Alteration of the DNA structure causes retardation in the migration of supercoiled DNA and a slight increase in the mobility of open circular DNA to a point where both forms comigrate. Interaction of the ruthenium(II) polypyridyl complexes containing α-amino acids on Topo II activity of the filarial parasite *S. cervi* was determined by enzyme-mediated supercoiled pBR322 relaxation assay [40,41]. Non-covalent interaction of protein with DNA is the key step in topoisomerase II catalytic cycle. Under physiological conditions, DNA replication repair, and transcription processes are significantly controlled by Topo II [42]. Anti-Topo II agents control Topo II activity either by trapping Topo II-DNA complex or acting as Topo II inhibitors [43]. DNA–metal interactions provided important informations about inhibitory effect of the metal complexes on Topo II activity of the filarial parasite. Gel electrophoresis shows that the ruthenium–tptz/tpy complexes imparting various α-amino acids (Figs. 7–9) display different modes of interaction with Topo II of *S. cervi.* Gel mobility assays of ruthenium(II) complexes (**4, 6, 10** and **13**) were examined at different concentration levels. Observed complex formation with the ruthenium–tptz/tpy complexes containing various α-amino acid series of complexes indicated that the complexes bind to Topo II-DNA complex, or DNA, or the enzyme. However, closely related complexes [Ru(κ^3-tptz)Cl_2(PPh_3)], and Ru(κ^3-tpy)(PPh_3)Cl_2], where both the labile chloro groups are replaced by amino acids, leads to relaxation of supercoiled DNA, with an inhibition percentage of 10–40%, where bulky PPh_3 and amino acid group destabilizes interaction with DNA strand. These results are consistent with other reports [44–47].

The complexes **4, 6, 10** and **13** exhibited strong complex formation at concentrations of 40 and 20 μg per reaction mixture with DNA topoisomerase of the filarial parasite (Fig. 7). The effect of these complexes at 10, 5 and 0.2 μg was also measured (Figs. 8 and 9). It was found that at these concentrations also, it showed complex formation as indicated by presence of DNA in the well. Further, reduction of the concentration to 0.2 μg led to a decrease in the complex intensity.

Extensive scientific attention has been paid towards anomalous morphology of Z-DNA and its involvement in gene expression and recombination [48,49]. Transition of the B–Z DNA in presence of complexes under study was followed spectrophotometrically. Complexes **4, 6, 10** and **13** were effective in causing conformational changes in DNA structure from B–Z transition. All other complexes also proved to have strong effect on DNA conversion (B–Z transition). The conformational changes in the structure of DNA from B–Z form is evidenced by observed change in the ratio A_{295}/A_{260}. An increase in the ratio of A_{295}/A_{260} from 0.18 (for free DNA) to 0.77(**3**), 0.66(**6**), 0.78(**7**) and 0.56(**13**) suggested destabilization of the DNA helix. Further, condensation of calf thymus CT DNA induced by the complexes was monitored spectrophotometrically by UV-absorption ratio of A_{320}/A_{260}. Above mentioned Ru(II) complexes showed enhancement in the absorption ratio at 320 nm [50,51]. All the complexes were found to cause condensation of DNA at 20 μg concentration. The condensation of DNA was monitored by measuring increase in the value of absorption at 320 nm [0.075 for free DNA to 0.38(**4**), 0.28(**6**), 0.45(**10**), and 0.53(**13**)].

The mononuclear ruthenium(II) polypyridyl complexes, **4**, **6**, **10**, and **13** also exhibited significant inhibitory effect on heme polymerase activity of *P. yoelii* lysate, which was studied by β-hematin formation [52]. The parent complex [Ru(κ^3-tptz)Cl_2(PPh_3)] showed 94% inhibition of heme polymerase activity while the complexes **4**, **6**, **10**, and **13** exhibited 50%, 50%, 54%, and 62% inhibition. The anomalous behavior of above result could be attributed to an increase in the steric hindrance by replacement of the chloro group in [Ru(κ^3-tptz)Cl_2(PPh_3)] and coordination of the amino acids to metal centre. All the complexes formed complex with DNA or caused condensation of DNA at concentration 20 μg or above per reaction mixture.

3. Experimental

3.1. Materials and physical measurements

Analytical grade chemicals were used through out. Solvents were dried and distilled before use following the standard

Table 3
Selected bond lengths and angles for complexes **6**, **10** and **13**.

Complex **6**		Complex **10**		Complex **13**	
Ru(1)–N(2)	1.936(4)	Ru(1)–(2)	1.951(5)	Ru(1)–N(2)	2.12(2)
Ru(1)–N(3)	2.090(5)	Ru(1)–N(3)	2.072(6)	Ru(1)–N(3)	1.94(2)
Ru(1)–N(1)	2.101(5)	Ru(1)–N(1)	2.075(6)	Ru(1)–N(1)	2.167(19)
Ru(1)–O(1)	2.109(4)	Ru(1)–O(1)	2.108(5)	Ru(1)–O(1)	2.116(17)
Ru(1)–N(7)	2.151(5)	Ru(1)–N(4)	2.139(5)	Ru(1)–N(4)	2.14(2)
Ru(1)–P(1)	2.3204(16)	Ru(1)–P(1)	2.3108(16)	Ru(1)–P(1)	2.317(5)
N(2)–Ru(1)–N(3)	79.07(19)	N(2)–Ru(1)–N(3)	79.9(3)	N(3)–Ru(1)–O(1)	171.0(7)
N(1)–Ru(1)–N(2)	78.70(18)	N(2)–Ru(1)–N(1)	79.4(2)	N(3)–Ru(1)–N(2)	79.4(3)
N(3)–Ru(1)–N(1)	156.99(17)	N(3)–Ru(1)–N(1)	158.5(2)	O(1)–Ru(1)–N(2)	103.7(7)
N(2)–Ru(1)–O(1)	172.16(17)	N(2)–Ru(1)–O(1)	170.81(18)	N(3)–Ru(1)–N(4)	81.1(8)
N(3)–Ru(1)–O(1)	100.77(17)	N(3)–Ru(1)–O(1)	101.7(2)	O(1)–Ru(1)–N(4)	95.7(7)
N(1)–Ru(1)–O(1)	100.44(16)	N(1)–Ru(1)–O(1)	97.84(19)	N(2)–Ru(1)–N(4)	160.1(8)
N(2)–Ru(1)–N(7)	93.39(18)	N(2)–Ru(1)–N(4)	93.0(2)	N(3)–Ru(1)–N(1)	158.6(3)
N(3)–Ru(1)–N(7)	87.9(2)	N(3)–Ru(1)–N(4)	85.4(2)	O(1)–Ru(1)–N(1)	78.1(6)
N(1)–Ru(1)–N(7)	87.5(2)	N(1)–Ru(1)–N(4)	89.9(2)	N(2)–Ru(1)–N(1)	90.8(8)
O(1)–Ru(1)–N(7)	78.78(16)	O(1)–Ru(1)–N(4)	78.1(2)	N(4)–Ru(1)–N(1)	88.6(7)
N(2)–Ru(1)–P(1)	93.34(13)	N(2)–Ru(1)–P(1)	94.66(15)	N(2)–Ru(1)–P(1)	87.7(6)
N(3)–Ru(1)–P(1)	91.15(14)	N(3)–Ru(1)–P(1)	94.12(16)	N(3)–Ru(1)–P(1)	92.7(6)
N(1)–Ru(1)–P(1)	95.98(14)	N(1)–Ru(1)–P(1)	93.35(15)	N(1)–Ru(1)–P(1)	173.5(6)
O(1)–Ru(1)–P(1)	94.49(12)	O(1)–Ru(1)–P(1)	94.25(12)	O(1)–Ru(1)–P(1)	96.0(4)
N(7)–Ru(1)–P(1)	172.90(13)	N(4)–Ru(1)–P(1)	172.08(17)	N(4)–Ru(1)–P(1)	94.9(5)

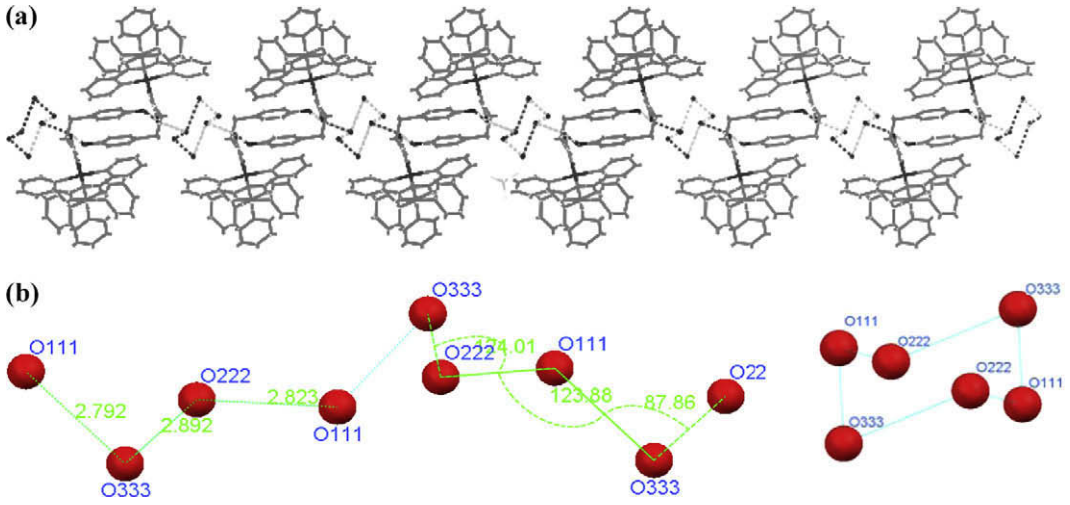

Fig. 6. (a) The two-dimensional sheet in complex **13** made up of one dimensional water chain. (b) Hydrogen-bonding motif of the self-assembled infinite water chain.

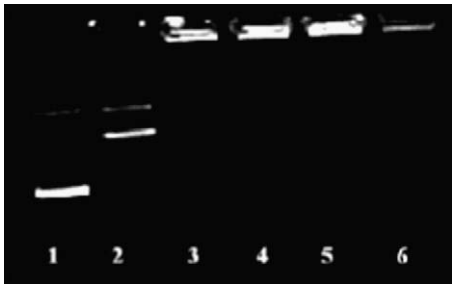

Fig. 7. Gel mobility shift assay of *S. cervi* topoisomerase II by complexes **4**, **6**, **10 and 13** (20 μg). Lane 1: pBR322 (0.25 μg) alone; lane 2: pBR322 + *S. cervi* Topo II; lane 3: **4**; lane 4: **6**; lane 5: **10**; lane 6: **13**.

literature procedures [53]. Hydrated ruthenium (III) chloride, 2,4,6-tris(2-pyridyl)-1,3,5-triazine (tptz), 2,2′:6′,2″-terpyridine (tpy), triphenylphosphine, ammonium tetrafluoroborate and amino acids (glycine, leucine, isoleucine, valine, tyrosine, proline and phenylalanine) were obtained from Aldrich Chemical Company, Inc., USA and were used without further purifications. The precursor complexes [Ru(κ^3-tptz)Cl_2(PPh_3)], [Ru(κ^3-tpy)Cl_2(PPh_3)] and [Ru(κ^3-tpy)Cl_3] were prepared and purified following the literature procedures [26,54]. Various buffers were prepared in triply distilled de-ionized water. Calf thymus (CT) DNA and supercoiled pBR322 DNA was procured from Sigma Chemical Co., St. Louis, MO. Topoisomerase II (Topo II) isolated from the filarial parasite *S. cervi* was partially purified following the literature procedures [55,56].

Microanalytical data on the complexes were provided by the microanalytical laboratory of the Sophisticated Analytical Instrument Facility, Central Drug Research Institute, Lucknow. Infrared spectra in nujol mull in the region 4000–400 cm^{-1} and electronic spectra were recorded on Shimadzu-8201 PC and Shimadzu UV-1601 spectrophotometers, respectively. ^1H and $^{31}P\{^1H\}$ NMR spectra at room temperature were obtained on a Bruker DRX-300 NMR machine. Electrochemical experiments were carried out in an airtight single compartment cell using platinum as the counter electrode, glassy carbon as the working electrode and Ag/Ag+ reference electrode on a CHI 620c electrochemical analyzer. Fast

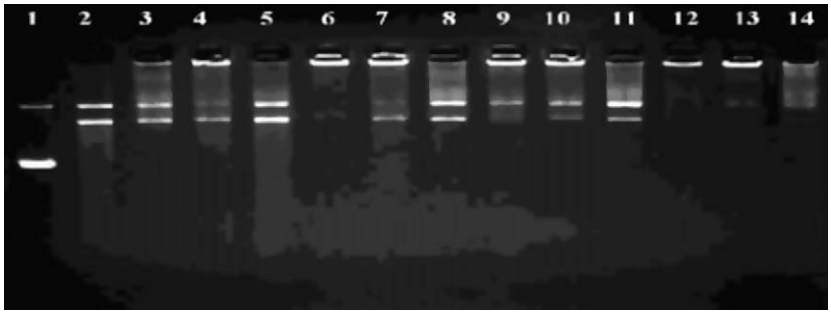

Fig. 8. Gel mobility shift assay of *S. cervi* topoisomerase II by complexes **4**, **6**, **10 and 13** (20 μg, lane 3, 6, 9, and 12; 10 μg, lane 4, 7, 10, and 13; 5 μg, lane 5, 8, 11, 14). Lane 1: pBR322 (0.25 μg) alone; lane 2: pBR322 + *S. cervi* Topo II; lanes 3–5: **4**; lanes 6–8: **6**; lanes 9–11: **10**, and lanes 12–14: **13**.

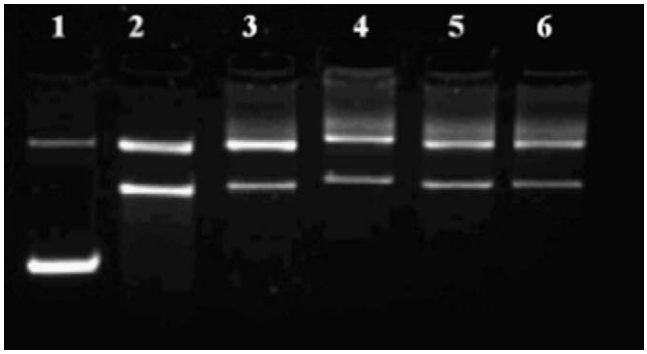

Fig. 9. Gel mobility shift assay of *S. cervi* topoisomerase II by complexes **4**, **6**, **10 and 13** (0.2 μg). Lane 1: pBR322 (0.25 μg) alone; lane 2: pBR322 + *S. cervi* Topo II; lane 3: **4**; lane 4: **6**; lane 5: **10**, and lane 6: **13**.

atom bombardment (FAB) mass spectra were recorded on a JOEL SX 102/ DA-6000 Mass spectrometer system using Xenon as the FAB gas (6 kV, 10 mA). The accelerating voltage was 10 kV and spectra were recorded at room temperature using *m*-nitrobenzyl alcohol as the matrix.

3.2. Syntheses

3.2.1. Preparation of [Ru(κ^3-tptz)(gly)(PPh_3)]BF_4 **3**

A suspension of [Ru(κ^3-tptz)Cl_2(PPh_3)] (0.746 g, 1.0 mmol) in methanol (25 ml) was treated with deprotonated solution of glycine (0.075 g, 1.0 mmol) and heated under reflux for four hours. Resulting purple solution was cooled to room temperature and filtered to remove any solid residue. The filtrate was concentrated under reduced pressure and a saturated solution of ammonium tetrafluoroborate dissolved in methanol was added to it and left for slow crystallization in refrigerator. Slowly, a microcrystalline product separated which was filtered, washed with diethyl ether and dried *in vacuo*. Yield: 0.463 g (62%). Anal. Calc. for $BC_{38}F_4H_{31}N_7O_2$PRu: C, 54.48; H, 3.70; N, 11.70. Found: C, 54.44; H, 3.72; N, 11.68%. ^{1}H NMR ($CDCl_3$, TMS, δ, ppm): 8.58 (d, 2H, J = 5.1 Hz), 8.38 (d, 2H, J = 7.8 Hz), 8.25 (d, 2H, J = 8.1 Hz), 7.98 (t, 2H, J = 7.8 Hz), 7.76 (t, 1H, J = 8.1 Hz), 7.54 (t, 2H, J = 6.3 Hz), 7.28–7.01 (br. m, 15H, PPh_3), 3.96 (s, 2H), 2.92 (s, 2H of $-NH_2$), ^{31}P{^{1}H} NMR ($CDCl_3$, H_3PO_4, δ, ppm): 39.18 (s). IR (cm^{-1}, nujol): $\nu(BF_4^-)$ 1052 cm^{-1}, $\nu(CO_s)$ 1398 cm^{-1}, $\nu(CO_{as})$ 1625 cm^{-1}. UV–Visible, λ_{max}, nm (ε): 238 (29 030), 282 (24 980), 354 (8330), 491 (7990)

3.2.2. Preparation of [Ru(κ^3-tptz)(leu)(PPh_3)]BF_4 **4**

The complex **4** was prepared from the reaction of [Ru(κ^3-tptz)Cl_2(PPh_3)] (0.746 g, 1.0 mmol) or [Ru(κ^3-tptz)(PPh_3)$_2$Cl]BF_4, with leucine (0.131 g, 1.0 mmol) in methanol under refluxing conditions, following the procedure for complex **3**. Yield: 0.624 g (83%). Anal. Calc. for $BC_{42}F_4H_{39}N_7O_2$PRu: C, 56.50; H, 4.37; N, 10.98. Found: C, 56.54; H, 4.40; N, 10.96%. ^{1}H NMR ($CDCl_3$, δ, ppm): 8.94 (d, 1H, J = 4.2 Hz), 8.72 (m, 5H), 7.96 (m, 3H), 7.55 (m, 3H), 7.32–7.13 (br. m, 15H, aromatic proton of PPh_3), 3.22 (d, 1H, J = 6.9 Hz), 2.0 (m, 1H), 1.39 (t, 2H, J = 10.2 Hz), 0.73 (dd, 6H, J = 6.6 Hz), 2.98 (s, 2H of $-NH_2$), ^{31}P{^{1}H} NMR ($CDCl_3$, H_3PO_4, δ, ppm): 40.08 (s). IR (cm^{-1}, nujol): $\nu(BF_4^-)$ 1060 cm^{-1}, $\nu(CO_s)$ 1382 cm^{-1}, $\nu(CO_{as})$ 1634 cm^{-1}. UV–Visible, λ_{max}, nm (ε): 240 (38 690), 281 (37 610), 350 (24 240), 487 (12 180).

3.2.3. Preparation of [Ru(κ^3-tptz)(isoleu)(PPh_3)]BF_4 **5**

The complex **5** was prepared from the reaction of [Ru(κ^3-tptz)Cl_2(PPh_3)] (0.746 g, 1.0 mmol) or [Ru(κ^3-tptz)(PPh_3)$_2$Cl]BF_4, with isoleucine(0.131 g, 1.0 mmol) in methanol following the procedure for complex **3**. Yield: 0.605 g (81%). Anal. Calc. for $BC_{42}F_4H_{39}N_7O_2$PRu: C, 56.50; H, 4.37; N, 10.98. Found: C, 56.34; H, 4.38; N, 10.94%. FAB-MS (obsd(calcd). rel intens, assignment): *m*/*z* 806 (806), 60, [Ru(κ^3-tptz)(isoleucine)(PPh_3)]$^+$; 675 (675), 50 [Ru(κ^3-tptz)(PPh_3)]$^{2+}$; 414 (414), 80 [Ru(κ^3-tptz)]$^{2+}$. ^{1}H NMR ($CDCl_3$, δ, ppm): 8.95 (d, 1H, J = 5.4 Hz), 8.71 (m, 5H), 7.94 (m, 3H), 7.57 (m, 3H), 7.26–7.16 (br. m, 15H, PPh_3), 3.50 (d, 1H, J = 10.5 Hz), 3.17 (m, 1H), 2.26 (m, 2H), 0.87 (m, 6H), ^{31}P{^{1}H} NMR ($CDCl_3$, H_3PO_4, δ, ppm): 39.88 (s). IR (cm^{-1}, nujol): $\nu(BF_4^-)$ 1055 cm^{-1}, $\nu(CO_s)$ 1394 cm^{-1}, $\nu(CO_{as})$ 1625 cm^{-1}. UV–Visible, λ_{max}, nm (ε): 237 (36 400), 276 (27 170), 356 (9420), 491 (9940).

3.2.4. Preparation of [Ru(κ^3-tptz)(val)(PPh_3)]BF_4 **6**

The complex **6** was prepared from the reaction of [Ru(κ^3-tptz)Cl_2(PPh_3)] (0.746 g, 1.0 mmol) or [Ru(κ^3-tptz)(PPh_3)$_2$Cl]BF_4, with valine (0. 117 g, 1.0 mmol) in methanol under refluxing conditions, following the procedure for complex **3**. Yield: 0.559 g (74%). Anal. Calc. for $BC_{41}F_4H_{37}N_7O_2$PRu: C, 56.04; H, 4.21; N, 11.16. Found: C, 56.06; H, 4.26; N, 11.10%. ^{1}H NMR ($CDCl_3$, δ, ppm): 8.90 (d, 1H, J = 7.2 Hz), 8.70 (m, 5H), 7.95 (m, 3H), 7.54 (m, 3H), 7.26–7.16 (br. m, 15H, PPh_3), 3.44 (d, 1H, J = 10.2 Hz), 3.13 (m, 1H), 0.86–0.76 (dd, 6H, J = 6.6 Hz), ^{31}P{^{1}H} NMR ($CDCl_3$, H_3PO_4, δ, ppm): 40.21 (s). IR (cm^{-1}, nujol): $\nu(BF_4^-)$ 1053, $\nu(CO_s)$ 1395, $\nu(CO_{as})$ 1633. UV–Visible, λ_{max}, nm (ε): 240 (35 440), 279 (34 780), 354 (10 770), 491 (12 080).

3.2.5. Preparation of [Ru(κ^3-tptz)(tyr)(PPh_3)]BF_4 **7**

The complex **7** was prepared from the reaction of [Ru(κ^3-tptz)Cl_2(PPh_3)] (0.746 g, 1.0 mmol) or [Ru(κ^3-tptz)(PPh_3)$_2$Cl]BF_4, with tyrosine (0.181 g, 1.0 mmol) in methanol under refluxing conditions, following the procedure for complex **3**. Yield: 0.586 g (78%). Anal. Calc. for $BC_{45}F_4H_{37}N_7O_3$PRu: C, 57.32; H, 3.92; N, 10.40. Found: C, 57.29; H, 3.95; N, 10.38%. FAB-MS (obsd(calcd). rel intens, assignment): *m*/*z* 856(856),70, [Ru(κ^3-tptz)(tyrosine)(PPh_3)]$^+$; 675 (675), 85 [Ru(κ^3-tptz)(PPh_3)]$^{2+}$; 414 (414),80 [Ru(κ^3-tptz)]$^{2+}$. ^{1}H NMR ($CDCl_3$, δ, ppm): 8.88 (d, 1H, J = 7.8 Hz), 8.70 (d, 1H, J = 7.8 Hz), 8.63 (d, 1H, J = 5.1 Hz), 8.55 (d, 1H,

J = 7.8 Hz), 8.35 (d, 1H, J = 7.5 Hz), 7.92 (m, 4H), 7.65 (d, 1H, J = 5.1 Hz), 7.48 (m, 2H), 7.12–7.02 (br. m, 15H, PPh_3), 6.88 (d, 2H, J = 7.8 Hz), 6.57 (d, 2H, J = 7.2 Hz), 3.56 (m, 1H, J = 7.8 Hz), 2.47 (m, 2H, J = 7.8 Hz), $^{31}P\{^1H\}$ NMR ($CDCl_3$, H_3PO_4, δ, ppm): 39.01 (s). IR (cm^{-1}, nujol): $\nu(BF_4^-)$ 1056, $\nu(CO_s)$ 1396, $\nu(CO_{as})$ 1621. UV–Visible, λ_{max}, nm (ε): 244 (39 060), 284 (39 170), 351 (16 000), 488 (17 500).

3.2.6. Preparation of [Ru(κ^3-tptz)(pro)(PPh_3)]BF_4 **8**

The complex **2f** was prepared from the reaction of [Ru(κ^3-tptz)Cl_2(PPh_3)] (0.746 g, 1.0 mmol) or [Ru(κ^3-tptz)(PPh_3)$_2$Cl]BF_4, with proline (0.115 g, 1.0 mmol) in methanol under refluxing conditions following the procedure for complex **3**. Yield: 0.613 g (82%). Anal. Calc. for $BC_{41}F_4H_{36}N_7O_2PRu$: C, 56.16; H, 4.11; N, 11.19. Found: C, 56.14; H 4.15,; N, 11.22%. ^1H NMR ($CDCl_3$, δ, ppm): 8.94 (d, 1H, J = 4.2 Hz), 8.72 (m, 5H), 7.98 (m, 3H), 7.54 (m, 3H), 7.26–7.12 (br. m, 15H, PPh_3), 3.76 (t, 1H, J = 8.4 Hz), 2.19 (t, 2H, J = 7.2 Hz), 1.45 (m, 4H), $^{31}P\{^1H\}$ NMR ($CDCl_3$, H_3PO_4,δ): 39.32 (s) ppm. IR (cm^{-1}, nujol): $\nu(BF_4^-)$ 1048 cm^{-1}, $\nu(CO_s)$ 1399 cm^{-1}, $\nu(CO_{as})$ 1639 cm^{-1}. UV–Visible, λ_{max}, nm (ε): 240 (37 680), 279 (35 160), 358 (12 910), 495 (14 860).

3.2.7. Preparation of [Ru(κ^3-tpy)(gly)(PPh_3)]BF_4 **9**

The complex **9** was prepared from the reaction of [Ru(κ^3-tpy)Cl_2(PPh_3)] (0.669 g, 1.0 mmol) with glycine (0.075 g, 1.0 mmol) in methanol under refluxing conditions, following the procedure for complex **3**. Yield: 0.423 g (63%). Anal. Calc. for $BC_{35}F_4H_{30}N_4O_2PRu$: C, 55.40; H, 3.96; N, 7.39. Found: C, 55.37; H, 3.98; N, 7.34%. ^1H NMR (DMSO, δ, ppm): 8.54 (d, 2H, J = 5.1 Hz), 8.30 (d, 2H, J = 7.8 Hz), 8.15 (d, 2H, J = 8.1 Hz), 7.95 (t, 2H, J = 7.8 Hz), 7.72 (t, 1H, J = 8.1 Hz), 7.54 (t, 2H, J = 6.3 Hz), 7.28–7.01(br. m, 15H, PPh_3), 3.96 (s, 2H), 2.93 (s, 2H of $-NH_2$), $^{31}P\{^1H\}$ NMR (DMSO, H_3PO_4, δ, ppm): 45.16 (s). IR (cm^{-1}, nujol): $\nu(BF_4^-)$ 1059 cm^{-1}, $\nu(CO_s)$ 1404 cm^{-1}, $\nu(CO_{as})$ 1612 cm^{-1}. UV–Visible, λ_{max}, nm (ε): 236 (27 720), 275 (14 040), 312 (20 990), 450 (2850), 500 (3940).

3.2.8. Preparation of [Ru(κ^3-tpy)(leu)(PPh_3)]BF_4 **10**

The complex **10** was prepared from the reaction of [Ru(κ^3-tpy)Cl_2(PPh_3)] (0.669 g, 1.0 mmol) with leucine (0.131 g, 1.0 mmol) in methanol under refluxing condition, following the procedure for complex **3**. Yield: 0.494 g (73%). Anal. Calc. for $BC_{39}F_4H_{38}N_4O_2PRu$: C, 57.56; H, 4.67; N, 6.89. Found: C, 57.51; H, 4.63; N, 6.88%. FAB-MS(obsd (calcd). rel intens, assignment): m/z 727 (727), 75, [Ru(κ^3-tpy)(leucine)(PPh_3)] $^+$; 596 (596), 80, [Ru(κ^3-tpy)(PPh_3)]$^{2+}$; 335 (335), 70, [Ru(κ^3-tpy)]$^{2+}$. ^1H NMR (Acetone, δ, ppm): 8.78 (m, 2H), 8.27 (t, 2H, J = 5.4 Hz), 8.13 (d, 2H, J = 6.3 Hz), 8.00 (m, 2H),7.77 (t, 1H, J = 7.8 Hz), 7.60 (t, 2H, J = 6.3 Hz), 7.30–7.18 (br. m, 15H, PPh_3), 3.37 (t, 1H, J = 6.6 Hz), 2.05 (m, 1H of ^{i}Pr), 1.36 (m, 2H), 0.66 (dd, 6H, J = 6.3 Hz), $^{31}P\{^1H\}$ NMR (Acetone, H_3PO_4, δ, ppm): 45.14 (s). IR (cm^{-1}, nujol): $\nu(BF_4^-)$ 1057 cm^{-1}, $\nu(CO_s)$ 1380 cm^{-1}, $\nu(CO_{as})$ 1625 cm^{-1}. UV–Visible, λ_{max}, nm (ε): 240 (36 960), 276 (27 070), 312 (35 760), 448 (5340), 497 (7630).

3.2.9. Preparation of [Ruκ^3-tpy)(isoleu)PPh_3)]BF_4 **11**

The complex **11** was prepared from the reaction of [Ru(κ^3-tpy)Cl_2(PPh_3)] (0.669 g, 1.0 mmol) with isoleucine (0.131 g, 1.0 mmol) in methanol under refluxing conditions following the procedure for complex **3**. Yield: 0.513 g (76%). Anal. Calc. for $BC_{39}F_4H_{38}N_4O_2PRu$: C, 57.56; H, 4.67; N, 6.89. Found: C, 57.58; H, 4.69; N, 6.81%. FAB-MS(obsd (calcd). rel intens, assignment): m/z 727(727), 60, [Ru(κ^3-tpy)(isoleucine)(PPh_3)]$^+$; 596 (596), 50, [Ru(κ^3-tpy)(PPh_3)]$^{2+}$; 334(334), 80 [Ru(κ^3-tpy)]$^{2+}$. ^1H NMR ($CDCl_3$, δ): 8.59 (d, 1H, J = 5.4 Hz), 8.51 (d, 2H, J = 5.9 Hz), 7.92 (t, 3H, J = 8.4 Hz), 7.78 (t, 4H, J = 7.8 Hz), 7.56 (t, 1H, J = 7.8 Hz), 7.33–7.09 (br. m, 15H, PPh_3), 3.23 (d, 1H, J = 10.5 Hz), 2.24 (m, 1H), 1.36 (m, 2H), 0.83 (m, 6H), $^{31}P\{^1H\}$ NMR ($CDCl_3$, H_3PO_4, δ, ppm): 44.22 (s). IR (cm^{-1}, nujol): $\nu(BF_4^-)$ 1060 cm^{-1}, $\nu(CO_s)$ 1382 cm^{-1}, $\nu(CO_{as})$ 1610 cm^{-1}. UV–Visible, λ_{max}, nm (ε): 235 (25 330), 275 (12 790), 312 (18 170), 449 (2630), 496 (3390).

3.2.10. Preparation of [Ru(κ^3-tpy)(val)(PPh_3)]BF_4 **12**

The complex **12** was prepared from the reaction of [Ru(κ^3-tpy)Cl_2(PPh_3)] (669 mg, 1.0 mmol) with valine (117 mg, 1 mmol) in methanol under refluxing condition, following the procedure for complex **3**. Yield: 0.537 g (80%). Anal. Calc. for $BC_{38}F_4H_{36}N_4O_2PRu$: C, 57.07; H, 4.50; N, 7.00. Found: C, 57.04; H, 4.54; N, 6.98%. ^1H NMR ($CDCl_3$, δ, ppm): 8.62 (d, 1H, J = 5.1 Hz), 8.55 (d, 1H, J = 4.8 Hz), 7.80 (m, 7H), 7.57 (t, 2H, J = 8.1 Hz), 7.29–7.09 (br. m, 15H, PPh_3), 3.10 (d, 1H, J = 6.7 Hz), 2.17 (m, 1H), 0.87 (d, 3H of ^{i}Pr, J = 7.2 Hz), 0.72 (d, 3H of ^{i}Pr, J = 6.9 Hz), $^{31}P\{^1H\}$ NMR ($CDCl_3$, H_3PO_4, δ, ppm): 43.67 (s). IR (cm^{-1}, nujol): $\nu(BF_4^-)$ 1062 cm^{-1}, $\nu(CO_s)$ 1379 cm^{-1}, $\nu(CO_{as})$ 1610 cm^{-1}. UV–Visible, λ_{max}, nm (ε):240 (37 500), 276 (23 050), 314 (31 200), 454 (426).

3.2.11. Preparation of [Ru(κ^3-tpy)(tyr)(PPh_3)]BF_4.3H_2O **13**

The complex **13** was prepared from the reaction of [Ru(κ^3-tpy)Cl_2(PPh_3)] (0.669 g, 1.0 mmol) with tyrosine (0.181 g, 1.0 mmol) in methanol under refluxing conditions following the procedure for complex **3**. Yield: 0.447 g (67%). Anal. Calc. for $BC_{48}F_4H_{36}N_4O_4PRu$: C, 60.58; H, 3.81; N, 5.89. Found: C, 60.54; H, 3.84; N, 5.84%. FAB-MS(obsd(calcd). rel intens, assignment): m/z 777 (777), 70 [Ru(κ^3-tpy)(tyrosine)(PPh_3)]$^+$; 596 (596), 85 [Ru(κ^3-tpy)(tyrosine)(PPh_3)];]$^{2+}$; 334 (334), 80 [Ru(κ^3-tpy)] $^{2+}$. ^1H NMR (Acetone, δ, ppm): 8.75 (d, 1H, J = 5.4 Hz), 8.30 (d, 1H, J = 5.4 Hz), 8.21 (t, 2H, J = 7.8 Hz), 8.06 (t, 2H, J = 5.4 Hz), 7.94 (m, 2H), 7.72 (t, 1H, J = 8.1 Hz), 7.55 (t, 1H, J = 6.6 Hz), 7.42 (t, 1H, J = 5.7 Hz), 7.31–7.15 (br. m, 15H, PPh_3), 6.85 (d, 2H, J = 8.4 Hz), 6.54 (d, 2H, J = 8.4 Hz), 4.12 (s, 2H, J = 6.3 Hz), 3.38 (d, 2H, J = 6.6 Hz), $^{31}P\{^1H\}$ NMR (Acetone, H_3PO_4, δ, ppm): 45.38 (s). IR (cm^{-1}, nujol): $\nu(BF_4^-)$ 1060 cm^{-1}, $\nu(CO_s)$ 1389 cm^{-1}, $\nu(CO_{as})$ 1602 cm^{-1}. UV–Visible, λ_{max}, nm (ε): 241 (38 600), 276 (32 940), 312 (37 820), 453 (6760), 500 (9500).

3.2.12. Preparation of [Ru(κ^3-tpy)(pro)(PPh_3)]BF_4 **14**

The complex **14** was prepared from the reaction of [Ru(κ^3-tpy)Cl_2(PPh_3)] (0.669 g, 1.0 mmol) with proline (0.115 g, 1.0 mmol) in methanol under refluxing conditions following the procedure for complex **3**. Yield: 0.518 g (77%). Anal. Calc. for $BC_{38}F_4H_{35}N_4O_2PRu$: C, 57.21; H, 4.39; N, 7.03. Found: C, 57.19; H, 4.36; N, 6.98%. ^1H NMR ($CDCl_3$, δ, ppm): 8.65 (d, 1H, J = 5.4 Hz), 8.50 (d, 1H, J = 5.4 Hz), 8.01 (d, 1H, J = 8.1 Hz), 7.72 (m, 7H), 7.63 (t, 1H, J = 8.1 Hz), 7.32–7.09 (br. m, 15H, PPh_3), 3.90 (t, 1H, J = 6.6 Hz), 3.63 (t, 2H, J = 8.7 Hz), 2.07 (m, 2H), 1.42 (m, 2H), $^{31}P\{^1H\}$ NMR ($CDCl_3$, H_3PO_4, δ, ppm): 43.30 (s). IR (cm^{-1}, nujol): $\nu(BF_4^-)$ 1063 cm^{-1}, ν_s(CO) 1379 cm^{-1}, ν_{as}(CO) 1611 cm^{-1}. UV–Visible, λ_{max}, nm (ε): 235 (25 550), 275 (12 620), 312 (18 120), 447 (2630), 499 (3390).

3.2.13. Preparation of [Ru(κ^3-tpy)(phe)(PPh_3)]BF_4 **15**

The complex **15** was prepared from the reaction of [Ru(κ^3-tpy)Cl_2(PPh_3)] (669 mg, 1.0 mmol) with phenylalanine (165 mg, 1 mmol) in methanol under refluxing conditions following the procedure for complex **3**. Yield: 0.565 g (84%). Anal. Calc. for $BC_{42}F_4H_{36}N_4O_2PRu$: C, 59.43; H, 4.24; N, 6.60. Found: C, 59.42; H, 4.26; N, 6.58%. ^1H NMR ($CDCl_3$, δ, ppm): 8.55 (d, 1H, J = 5.1 Hz), 7.91 (d, 1H, J = 7.8 Hz), 7.74 (m, 7H), 7.61 (t, 1H, J = 7.8 Hz), 7.51 (t, 1H, J = 8.1 Hz), 7.26–7.04 (br. m, 15H, PPh_3, and 4H of Ph ring of phenylalanine), 6.87 (t, 1H, J = 6.3 Hz), 3.88 (t, 1H, J = 10.2 Hz), 3.64 (d, 2H, J = 13.2 Hz), 2.11 (s, 2H of H_2N–) $^{31}P\{^1H\}$ NMR ($CDCl_3$, H_3PO_4, δ, ppm): 44.02 (s). IR (cm^{-1}, nujol): $\nu(BF_4^-)$ 1056 cm^{-1}, $\nu(CO_s)$ 1380 cm^{-1}, $\nu(CO_{as})$ 1627 cm^{-1}. UV–Visible, λ_{max}, nm (ε): 241 (38 800), 276 (35 540), 312 (38 900), 452 (7530), 497 (10 120).

3.3. X-ray crystallography

Suitable crystals for X-ray diffraction analyses for complexes **6**, **10** and **13**, were obtained from slow diffusion of CH_2Cl_2/petroleum ether (40–60 °C) at room temperature. Preliminary data on the space group and unit cell dimensions as well as intensity data were collected on an OXFORD DIFFRACTION XCAUBER-S' and Bruker Smart Apex diffractometer using graphite-monochromatized Mo Kα radiation .The structures were solved by direct methods and refined by using SHELX-97 [57]. The non-hydrogen atoms were refined with anisotropic thermal parameters. All the hydrogen atoms are geometrically fixed and allowed to refine using a riding model. The computer program PLATON was used for analyzing the interaction and stacking distances [58].

3.4. Gel mobility shift assay

Interaction of the complexes with DNA Topo II was governed by enzymatic-mediated super coiled pBR322 relaxation [35]. For the relaxation of super coiled pBR322 DNA a reaction mixture (20 μl) containing 50 mM Tris–HCl, pH 7.5, 50 mM KCl, 1 mM $MgCl_2$ 1 mM ATP, 0.1 mM EDTA, 0.5 mM DTT, 30 μg/ml BSA and enzyme protein was employed. Super coiled pBR322 DNA (0.25 μg) was used as the substrate for above reaction mixture. The reaction mixture was incubated for 30 min at 37 °C and stopped by addition of 5 μl of the loading buffer containing 0.25% bromophenol blue, 1 M sucrose, 1 mM EDTA, and 0.5% SDS. Samples were applied on horizontal 1% agarose gel in 40 mM tris acetate buffer, pH 8.3, and 1 mm EDTA and run for 10 h at room temperature at 20 V. The gel was stained with ethidium bromide (0.10 μg/ml) and photographed in a GDS 7500 UVP (Ultra Violet Product, Cambridge, UK) trans-illuminator. One unit of topoisomerase activity is defined as the amount of enzyme required to relax 50% of the super coiled DNA under the standard assay conditions.

The conformational transitions of B to Z in CT DNA in the presence of mononuclear ruthenium complexes were determined spectrophotometrically .[48,49]. The UV absorbance ratio A_{295}/A_{260} was monitored for conformational change in the DNA helix from B–Z DNA. Condensation of DNA was monitored by following the increase in the value of absorbance at 320 nm against different complex/DNA ratios, according to the method of Basu and Marton [50].

3.5. Heme polymerase assay

Inhibition of *P. yoelii* lysate heme polymerase activity by mononuclear ruthenium complexes was studied by measuring the beta hematin formation as reported previously [52]. For determining the inhibition percentage of anti-malarial activity, the reaction mixture (1 ml) contained 100 μl of 1 M sodium phosphate buffer, 20 μl of hemin (1.2 mg/ml), and 25 μl of *P. yoelii* enzyme, and the volume was made up with triple-distilled water. A total of 20 μg of the complexes were added in the reaction mixture and incubated for 16 h at 37 °C in an incubator shaker at the speed of 174 rpm. After incubation, the reaction mixture was centrifuged at 10 000 rpm for 15 min and the pellet obtained was washed three times with 10 ml of buffer containing 0.1 M Tris–HCl buffer, pH 7.5, and 2.5% SDS and then with buffer 2 (0.1 M sodium bicarbonate buffer, pH 9.2, and 2.5% SDS), followed by distilled water. The semi-dried pellets were suspended in 50 μl of 0.2 N NaOH and the volume was adjusted to 1 ml with distilled water. The optical density was measured at 400 nm and the percent inhibition was calculated using the following formula:

$$\%\ \text{inhibition} = (1 - \text{o.d of control})/\text{o.d of experimental} \times 100$$

4. Conclusions

Through this study we have shown that the syntheses of complexes containing both a polypyridyl ligand tptz/tpy or bio-relevant ligands, α-amino acids can be achieved by reactions of $Ru(\kappa^3\text{-tptz})Cl_2(PPh_3)$, and $Ru(\kappa^3\text{-tpy})Cl_3$ with α-amino acids. Resulting complexes moderately interact with DNA causing condensation and exhibit inhibitory activity against DNA Topo II of the filarial parasite S. *cervi* at higher concentrations by complex formation with DNA. These also exhibit heme polymerase activity against malarial parasite P. *yoelii*.

Acknowledgements

We gratefully acknowledge the support of the Department of Science and Technology, Ministry of Science and Technology, New Delhi, India (grant SR/SI/IC-15/2007) for providing financial assistance and Prof. P. Mathur, In-charge, National Single Crystal X-ray Diffraction Facility, Indian Institute of Technology, Bombay, Mumbai, for providing single X-ray data. We also thank Miss Rima Ray Sarkar, Central Drug Research Institute, India for technical support regarding Topo II activity.

Appendix A. Supplementary material

CCDC 710601, 710602 and 710603 contain the supplementary crystallographic data for **6**, **10** and **13**. These data can be obtained free of charge from The Cambridge Crystallographic Data Centre via www.ccdc.cam.ac.uk/data_request/cif. Supplementary data associated with this article can be found, in the online version, at doi:10.1016/j.jorganchem.2009.07.014.

References

[1] V. Balzani, A. Juris, M. Venturi, S. Campagna, F. Puntariero, S. Serroni, Coord. Chem. Rev. 96 (1996) 759.
[2] K. Chichak, U. Jacquemard, N.R. Branda, J. Eur. Inorg. Chem. (2002) 357.
[3] Xue W. Liu, Jun Li, Hong Deng, Kang C. Zheng, Zong W. Mao, Liang N. Ji, Inorg. Chim. Acta 358 (2005) 3311.
[4] A. Cindy Puckett, K. Jacqueline Barton, J. Am. Chem. Soc. 129 (2007) 46.
[5] N. Maribel, B. Adelmo, H. Clara, M. Edgar, J. Braz. Chem. Soc. (2008) 1355.
[6] C.J. Elsevier, J. Reedijk, P.H. Walton, M.D. Ward, Dalton Trans. (2003) 1869.
[7] K.D. Demadis, C.M. Hartshorn, T.J. Meyer, Chem. Rev. 101 (2001) 2655.
[8] M.I.J. Polson, E.A. Medlycott, G.S. Hanan, L. Mikelsons, N.J. Taylor, M. Watanabe, Y. Tanaka, F. Loiseau, R. Passalacqua, S. Campagna, Chem. Eur. J. 10 (2004) 3640.
[9] C.M. Metcalfe, S. Spey, H. Adams, J.A.J. Thomas, Chem. Soc., Dalton Trans. (2002) 4732.
[10] A. Amboise, B.J. Maiya, Inorg. Chem. 39 (2000) 4256.
[11] X.-J. Yang, F. Drepper, B. Wu, W. Sun, W. Haehnel, C. Janiak, Dalton Trans. (2005) 256.
[12] K. Karidi, A. Garoufis, N. Hadjiliadis, J. Reedijik, Dalton Trans. (2005) 256.
[13] F. Gao, H. Chao, L.N. Ji, Chem. Biodiv. Rev. 5 (2008) 1962.
[14] A. Sitlani, C.M. Dupureur, J.K. Barton, J. Am. Chem. Soc. 115 (1993) 12589.
[15] K. Weise, Angew. Chem., Int. Ed. 36 (2003) 2592.
[16] G. Ciancaleoni, I.D. Maio, D. Zuccaccia, A. Macchioni, Organometallics 26 (2007) 489.
[17] M.L. Gonzalez, J.M. Tercero, A. Matilla, J. Niclos-Gutirrez, M.T. Fernandez, M.C. Lopez, C. Alonso, S. Gonalez, Inorg. Chem. 36 (1997) 1806.
[18] A. Matilla, J.M. Tercero, N.H. Dung, B. Viossat, J.M. Perez, C. Alonso, J.D. Martin-Ramos, J. Niclos-Gutirrez, J. Inorg. Biochem. 55 (1994) 235.
[19] T.G. Appleton, Coord. Chem. Rev. 166 (1997) 313.
[20] H. Kozlowski, L.D. Pettit, F.R. Hartley (Eds.), Chemistry of Platinum Group Metals: Recent Developments, Elsevier, Amsterdam, 1991, p. 530.
[21] L.J.K. Boerner, J.M. Zaleski, Curr. Opin. Chem. Biol. 9 (2005) 135.
[22] R.L. William, H.N. Toft, B. Winkel, K.J. Brewer, Inorg.Chem. 42 (2003) 4394.
[23] M. Sironi, Mol. Biochem. Parasitol. 74 (1995) 223.
[24] S.K. Singh, S. Sharma, M. Chandra, D.S. Pandey, J. Organomet. Chem. 690 (2005) 3130.
[25] P. Paul, B. Tyagi, A.K. Bilakhiya, P. Dastidar, E. Suresh, Inorg. Chem. 39 (2000) 14.
[26] S. Sharma, S.K. Singh, D.S. Pandey, Inorg. Chem. 47 (2008) 1179.
[27] C. Djordjevic, N. Vuletic, B.A. Jacobs, M. Lee-Reenslo, E. Sinn, Inorg. Chem. (1997) 36.
[28] J. Goubean, W.Z. Bues, Anorg. Allg. Chem. 268 (1952) 221.

[29] N.N. Greenwood, J. Chem. Soc. (1959) 3811.
[30] S. Chirayil, V. Hegde, Y. Jahng, R.P. Thummel, Inorg. Chem. 30 (1991) 2821.
[31] K. Majumder, R.J. Butcher, S. Bhattacharya, Inorg. Chem. 41 (2002) 4605.
[32] C. Metcalfe, S.D. Spey, H. Adam, J.A. Thomas, Dalton Trans. (2002) 4732.
[33] M.H.V. Huynh, D.G. Lee, P.S. White, T.J. Mayer, Inorg. Chem. 40 (2001) 3842.
[34] D. Braga, F. Grepioni, E. Tedesco, Organometallics 17 (1998) 2669.
[35] J.H.K.K. Hirschberg, L. Brunsveld, A. Ramzi, J.A.J.M. Vekemans, R.P. Sijbesma, E.W. Meijer, Nature 407 (2000) 167.
[36] H. Yin, G.I. Lee, H.S. Park, G.A. Payne, J.M. Rodriguez, S.M. Sebti, A.D. Hamilton, Angew. Chem., Int. Ed. 44 (2005) 2704.
[37] G.A. Jeffrey, An Introduction to Hydrogen Bonding, Oxford University Press, Oxford, UK, 1997. p. 160.
[38] K. Liu, M.G. Brown, C. Carter, R.J. Saykally, J.K. Gregory, D.C. Clary, Nature 381 (1996) 501.
[39] M. Matsumoto, S. Saito, I. Ohmine, Nature 416 (2002) 409.
[40] U. Pandya, J.K. Saxena, S.M. Kaul, P.K. Murthy, R.K. Chatterjee, R.P. Tripathi, A.P. Bhaduri, O.P. Shukla, Med. Sci. Res. 27 (1999) 103.
[41] D.A. Burden, N. Osheroff, Biochim. Biophys. Acta 1400 (1998) 139.
[42] J.C. Wang, J. Biol. Chem. 266 (1991) 6659.
[43] R.E. Morris, R.E. Aird, P. del S.Murdoch, H. Chen, J. Cummings, N.D. Hughes, S. Parsons, A. Parkin, G. Boyd, D.I. Jodrell, P.J. Sadler, J. Med. Chem. 44 (2001) 3616.
[44] W.H. Ang, P.J. Dyson, J. Eur. Inorg. Chem. (2006) 4003.
[45] D.V. Deubel, J.K.C. Lau, Chem. Commun. (2006) 2451.
[46] C. Scalaro, A. Bergamo, L. Brescacin, G. Sava, P.J. Dyson, J. Med. Chem. 48 (2005) 4161.
[47] B. Serli, E. Zangrando, T. Gianferrara, C. Scalaro, P.J. Dyson, A. Bergamo, E. Alessio, J. Eur. Inorg. Chem. (2005) 3423.
[48] E.M. Pohl, T.M. Jovin, J. Mol. Biol. 67 (1972) 375.
[49] J.B. Chaires, J. Biol. Chem. 261 (1986) 8899. and references therein.
[50] H.S. Basu, L.J. Marton, Biochem. J. 244 (1987) 243.
[51] T.J. Thomas, R.P.J. Messner, Mol. Biol. 201 (1988) 463.
[52] A.V. Pandey, N. Singh, B.L. Takwani, S.K. Puri, V.S. Chauhan, J. Pharma. Biomed. Anal. 20 (1999) 203.
[53] D.D. Perrin, W.L.F. Armango, D.R. Perrin, Purification of Laboratory Chemicals, Pergamon, Oxford, UK, 1986.
[54] B.P. Sullivan, M.C. Jaffrey, T.J. Meyer, Inorg. Chem. 19 (1980) 1404.
[55] G.R. Desiraju, T. Steiner, Weak Hydrogen Bonds in Structural Chemistry and Biology, Oxford University Press, Oxford, UK, 1999.
[56] T. Steiner, Angew. Chem., Int. Ed. 41 (2002) 48.
[57] G.M. Sheldrick, SHELX-97: Programme for the Solution and Refinement of Crystal Structures, University of Göttingen, Germany, 1997.
[58] A.L. Spek, Acta Crystallogr. 46 (1990) C31.